

Journal Pre-proof



Molecular and physiological analysis of indole-3-acetic acid degradation in *Bradyrhizobium japonicum* E109

Daniela Torres, Elías Mongiardini, Florencia Donadío, Raúl Donoso, Gonzalo Recabarren-Gajardo, José Gualpa, Stijn Spaepen, Roberto Defez, Gastón Lopez, Carmen Bianco, Fabricio Cassán

PII: S0923-2508(21)00027-9

DOI: <https://doi.org/10.1016/j.resmic.2021.103814>

Reference: RESMIC 103814

To appear in: *Research in Microbiology*

Received Date: 27 August 2020

Revised Date: 20 January 2021

Accepted Date: 26 January 2021

Please cite this article as: D. Torres, E. Mongiardini, F. Donadío, R. Donoso, G. Recabarren-Gajardo, J. Gualpa, S. Spaepen, R. Defez, G. Lopez, C. Bianco, F. Cassán, Molecular and physiological analysis of indole-3-acetic acid degradation in *Bradyrhizobium japonicum* E109, *Research in Microbiology*, <https://doi.org/10.1016/j.resmic.2021.103814>.

This is a PDF file of an article that has undergone enhancements after acceptance, such as the addition of a cover page and metadata, and formatting for readability, but it is not yet the definitive version of record. This version will undergo additional copyediting, typesetting and review before it is published in its final form, but we are providing this version to give early visibility of the article. Please note that, during the production process, errors may be discovered which could affect the content, and all legal disclaimers that apply to the journal pertain.

© 2021 Institut Pasteur. Published by Elsevier Masson SAS. All rights reserved.

1 **Molecular and physiological analysis of indole-3-acetic acid degradation in**
2 ***Bradyrhizobium japonicum* E109**

3

4 **Daniela Torres^a, Elías Mongiardini^b, Florencia Donadío^a, Raúl Donoso^{c,d}, Gonzalo**
5 **Recabarren-Gajardo^{e,f}, José Gualpa^a, Stijn Spaepen^g, Roberto Defez^h, Gastón**
6 **Lopez^{a,1}, Carmen Bianco^{h,1}, Fabricio Cassán^{a,1}**

7

8 ^aInstituto de Investigaciones Agrobiotecnológicas (INIAB). Universidad Nacional de Río
9 Cuarto, Córdoba Argentina

10 ^bLaboratorio de Interacciones Rizobios y Soja. Instituto de Biotecnología y Biología
11 Molecular. Facultad de Ciencias Exactas. Universidad Nacional de La Plata, La Plata,
12 Argentina

13 ^cPrograma Institucional de Fomento a la Investigación, Desarrollo e Innovación (PIDi),
14 Universidad Tecnológica Metropolitana, Santiago, Chile

15 ^dCenter of Applied Ecology and Sustainability (CAPES), Santiago, Chile

16 ^eBioactive Heterocycles Synthesis Laboratory, BHSL, Departamento de Farmacia,
17 Facultad de Química y de Farmacia, Pontificia Universidad Católica de Chile, Santiago,
18 Chile

19 ^fCentro Interdisciplinario de Neurociencias, Pontificia Universidad Católica de Chile,
20 Santiago, Chile

21 ^gKatholieke Universiteit Leuven. Leuven, Belgium.

22 ^hInstitute of Biosciences and Bioresources, National Research Council of Italy, UOS
23 Naples, Italy

24

25 *Correspondence: fcassan@exa.unrc.edu.ar; Tel.: +54-9-358-4676-532

26 ¹ Cassán Fabricio, Carmen Bianco and López Gastón have contributed equally to this work.

27 E-mail addresses: dtorres@exa.unrc.edu.ar (Daniela Torres), Elías Mongiardini
28 (mongiardini@biol.unlp.edu.ar), fdonadio@exa.unrc.edu.ar (Florencia Donadío),
29 radonoso@uai.cl (Raúl Donoso), grecabarren@uc.cl (Gonzalo Recabarren-Gajardo),
30 jgualpa@exa.unrc.edu.ar (Jose Gualpa), glopez@exa.unrc.edu.ar (Gastón Lopez),
31 roberto.defez@ibbr.cnr.it (Roberto Defez), carmen.bianco@ibbr.cnr.it (Carmen Bianco),
32 fcassan@exa.unrc.edu.ar (Fabricio Cassán).

33

34

35 **Abstract**

36 *Bradyrhizobium japonicum* E109 is a bacterium widely used for inoculants production in
37 Argentina. It is known for its ability to produce several phytohormones and degrade
38 indole-3-acetic acid (IAA). The genome sequence of *B. japonicum* E109 was recently
39 analyzed and it showed the presence of genes related to the synthesis of IAA by
40 indole-3-acetonitrile, indole-3-acetamide and tryptamine pathways. Nevertheless, *B.*
41 *japonicum* E109 is not able to produce IAA and instead has the ability to degrade this
42 hormone under saprophytic culture conditions. This work aimed to study the molecular
43 and physiological features of IAA degradation and identify the genes responsible of this
44 activity. In *B. japonicum* E109 we identified two sequences coding for a putative
45 3-phenylpropionate dioxygenase (subunits α and β) responsible for the IAA degradation
46 that were homologous to the canonical cluster of *iacC* and *iacD* of *P. putida* 1290. These
47 genes form a separate cluster together with three additional genes with unknown
48 functions. The degradation activity was found to be constitutively expressed in *B.*
49 *japonicum* E109. As products of IAA degradation, we identified two compounds,
50 3-indoleacetic acid 2,3-oxide and 2-(2-hydroperoxy-3-hydroxyindolin-3-yl) acetic acid.
51 Our report proposes, for the first time, a model for IAA degradation in *Bradyrhizobium*.

52

53 **Keywords:** *B. japonicum*; indole-3-acetic acid; IAA; 3-phenylpropionate dioxygenase;
54 3-indoleacetic acid 2;3-Oxide; 2-(2-hydroperoxy-3-hydroxyindolin-3-yl) acetic acid

55

56 1. Introduction

57 The auxins are a group of phytohormones characterized by their ability to induce
58 plant growth and to reproduce the physiological effects of the naturally occurring
59 indole-3-acetic acid (IAA). The IAA metabolism in higher plants, fungi and bacteria
60 comprises several mechanisms, such as the biosynthesis, degradation, catabolism (i.e.
61 oxidation and assimilation), conjugation and hydrolysis of auxin conjugates [1], which
62 globally regulate the IAA levels in these biological systems. *Bradyrhizobium* is an
63 alphaproteobacterium with the ability to produce IAA and this capacity has been
64 demonstrated *in vitro* and *in planta* after soybean inoculation [2-4]. Thimann [5]
65 proposed that auxins play an important role in the ontogeny of the root nodules during the
66 rhizobia-legume symbiosis, as many studies have indicated that a change in the
67 concentration of this phytohormone is a pre-requisite for nodule organogenesis [6].
68 Nielsen et al. [7] were the first to report that *B. diazoefficiens* USDA110 (formerly *B.*
69 *japonicum* USDA110) has the capacity to degrade indole-3-acetic acid (IAA) and Egebo
70 et al. [8] suggested that this reaction might be dependent on oxygen availability in the
71 culture medium. Jensen et al. [9] isolated metabolites of IAA degradation in *B.*
72 *diazoefficiens* USDA110 and the identified products suggested a new metabolic pathway
73 that included anthranilic acid. However, they could not confirm this pathway or identify
74 the gene(s) or enzyme(s) responsible for such capacity.

75 Two sets of canonical genes have been characterized for IAA catabolism in bacteria:

76 i) the *iac* (indole 3-acetic acid catabolism) gene cluster identified in *P. putida* 1290 [10]

77 and others bacteria, which codes for an aerobic pathway through which IAA is
78 transformed into catechol; the *iaa* (indole 3-acetic acid degradation) gene cluster
79 identified in *Aromatoleum aromaticum* EbN1 [11], which underlies the anaerobic
80 conversion of IAA into 2-aminobenzoyl-CoA. *P. putida* 1290 has the ability to degrade
81 IAA as the sole source of carbon and energy (catabolism). This process is carried out by
82 the *iac* locus, which consists of 10 genes coding for enzymes with a metabolic activity for
83 both indole and aromatics molecules, as well as proteins with regulatory functions [10].
84 At present, there is no information about the full set of processes involved in the IAA
85 catabolism in *B. japonicum*, its homeostatic control, or the effects on the symbiotic
86 interaction with soybean. *B. japonicum* E109 has been one of the most used strains for the
87 production of soybean inoculants in Argentina for 40 years [12]. The genome sequence of
88 *B. japonicum* E109 has revealed the presence of genes involved in several plant growth
89 promoting mechanisms and in particular in the biosynthesis of the phytohormone IAA
90 [13]. The genome analysis of E109 revealed the existence of three putative pathways for
91 IAA biosynthesis: indole-3-pyruvate (IPyA), indole-3-acetonitrile (IAN) and
92 indole-3-acetamide (IAM) [14]. However, the LC-MS-MS analysis did not show
93 significant amounts of the hormone in liquid culture media, suggesting that *B. japonicum*
94 E109 is not able to produce IAA, but on the contrary it has the ability to degrade IAA
95 under *in vitro* conditions [15]. In the same report, we also confirmed the ability of *B.*
96 *japonicum* E109 to degrade other natural and synthetic auxins, such as indole-3-butyric
97 acid (IBA) or α -naphthalene acetic acid (NAA). Exogenous IAA induced an increase in
98 the production of biomass and exopolysaccharide in liquid culture media of *B. japonicum*
99 E109, leading to a modification of its symbiotic behavior with soybean plants.

100 The aim of this work was to analyze the molecular and physiological features of IAA
101 degradation in *B. japonicum* E109 in order to identify the responsible genes and the
102 produced metabolites, and to outline a putative degradation pathway in this bacterium.

103

104 **2. Materials and Methods**

105 **2.1 Bacterial strains and culture conditions**

106 The strains and their characteristics are summarized in Table 1. *B. japonicum* E109
107 (*Bj*E109) was provided by the IMYZA-INTA, Buenos Aires (Argentina); *B. elkanii*
108 SEMIA5019 (*Be*SEMIA5019) was obtained from Empresa Brasileira de Pesquisa
109 Agropecuaria (EMBRAPA) in Brazil; *B. diazoefficiens* USDA110 wild type
110 (*Bd*USDA110) and *B. diazoefficiens* USDA110 deficient in *nrgC* gene named *B.*
111 *diazoefficiens* 8620 or USDA110 *spc4* (*Bd*USDA110 Δ *iacA*) were provided by Prof. Dr.
112 Hans-Martin Fischer of Institute of Microbiology in Zürich, Switzerland. Despite the
113 product of *nrgC* (*NrgC*, accession number AAG61032) has been previously associated
114 with nitrogen fixation [16], *in silico* analysis showed that *nrgC* sequence has homology
115 with that of *iacA* of *P. putida* 1290, related with IAA degradation [10] and *idoA* of *P.*
116 *alcaligenes* PA-10 related with indigo production [17]. Thus this strain was named as
117 *Bd*USDA110 Δ *iacA* in Table 1 and along the manuscript. Bacteria were inoculated in
118 250 ml flasks containing 100 ml of Yeast Extract Mannitol (YEM) culture medium [21]
119 modified by the addition of 10 mg.l⁻¹ L-tryptophan (Trp) as the main precursor for IAA
120 biosynthesis [22] and antibiotics according to the strain (Table 1). Cultures were
121 incubated at 30°C with orbital shaking (180 rpm) until exponential growth phase was

122 reached. The purity of the cultures was checked routinely on YEM agar [21] and TSA
123 plating (Trypticase Soybean Agar) at 10% (v/v).

124

125 **Table 1**

126

127 **2.2 IAA degradation by *Bradyrhizobium***

128 We compared the IAA degradation activity in three strains belonging to different
129 species of *Bradyrhizobium* according to Torres et al. [15]. In particular, 100 μ l aliquots
130 obtained from exponential growth phase cultures of *BjE109*, *BeSEMIA5019* and
131 *BdUSDA110* were individually inoculated in 250 ml flasks containing 100 ml of YEM
132 culture medium [21] modified by the addition L-Trp as described before. Cultures were
133 incubated at 30°C with orbital shaking (180 rpm) until early exponential growth phase
134 ($OD_{595} \approx 0.6$), and were divided into 5 ml aliquots which were dispensed into 10 ml sterile
135 borosilicate tubes. After 15 min of incubation conditions at 30°C, 200 μ l of 1 $\text{mg}\cdot\text{ml}^{-1}$
136 IAA solution (or equivalent volume of sterilized water) were separately added into the
137 tubes containing the cultures of each strain to obtain a final concentration $\approx 40 \mu\text{g}\cdot\text{ml}^{-1}$
138 ($38.5 \mu\text{g}\cdot\text{ml}^{-1}$) IAA per tube. This concentration was selected because it is similar to that
139 produced by several rhizobacteria, including the phytostimulatory model *Azospirillum*
140 *brasilense* [22]. To account for the non-biological degradation of the compound the same
141 volume of IAA solution was added to tubes containing 5 ml of non-inoculated YEM
142 medium. Tubes were incubated at 30°C with orbital shaking (180 rpm) and samples were
143 taken at T0 (5-10 min after IAA induction) and every 2 h to measure the IAA
144 concentration ($\mu\text{g}\cdot\text{ml}^{-1}$).

145

146 **2.3 Quantification of IAA**

147 Quantification of IAA was performed by spectrophotometry [23] and confirmed by
148 HPLC according to Torres et al. [15]. Briefly, aliquots of 500 μl of bacterial culture were
149 centrifuged at 11.300 x g for 10 min. Subsequently, 250 μl of supernatant was filtered
150 (0.2 μm), mixed with 250 μl of Salkowski's reagent (7.9 M H_2SO_4 and 12.5 g l^{-1} FeCl_3)
151 and gently shaken in inverted position at least 10 times. Samples were incubated in the
152 dark for 30 min and the absorbance at 530 nm was measured. An aliquot of filtered
153 supernatants was also injected with a final volume of 20 μl in an HPLC Waters 600-MS
154 device (Waters Inc., USA) equipped with an U6K injector and C18 reverse phase column
155 (Purospher STAR RP C-18, 3 mm, Lichrocart 55-4) heated at 30 $^\circ\text{C}$, coupled to a system
156 with UV-VIS Waters 486 detector (Waters Inc., USA) set at 265 nm. The elution was
157 performed with a mixture of ethanol: acetic acid: water (Et-OH/H-Ac/H₂O) (12: 1: 87) as
158 mobile phase at a flow rate of 1 $\text{ml}\cdot\text{min}^{-1}$ at 30 $^\circ\text{C}$. The retention time for IAA was
159 10.1-10.3 minutes and it was previously identified using an appropriate standard solution
160 of IAA (Sigma Aldrich, Germany). Quantification was performed by integration of the
161 peak area corresponding to the retention time (RT) using an integration software (Waters
162 Inc. USA). The IAA concentration was expressed in $\mu\text{g}\cdot\text{ml}^{-1}$

163

164 **2.4 Analysis of constitutive or inducible character of IAA degradation**

165 We evaluated whether the degradation of IAA was triggered by its own addition
166 (inducible) or it depended on bacterial growth (constitutive). For that, *BjE109* was grown
167 until late exponential growth phase ($\text{OD}_{595}=1.2$), then a 50 ml aliquot was centrifuged at
168 8000 rpm for 15 min, and the cell-free supernatant was filtered (0.2 μm). The resultant
169 filtrate was divided into 5 ml aliquots and transferred into 10 ml sterile borosilicate tubes
170 for IAA induction. The treatments of the supernatants were the following: (1) addition of

171 IAA solution to obtain a final concentration $\approx 40 \mu\text{g}\cdot\text{ml}^{-1}$ IAA per tube (sE109); (2)
172 addition of IAA to heat denatured supernatants (15 min at 90°C) to obtain a final
173 concentration $\approx 40 \mu\text{g}\cdot\text{ml}^{-1}$ IAA per tube (sE109 ϕ) and (3) addition of 200 μl of sterile
174 water to supernatants, and (4) addition of 200 μl of sterile water to denatured
175 supernatants. Tubes were incubated as previously described and 500 μl of the mixtures
176 were sampled every 2 h to measure IAA concentration ($\mu\text{g}\cdot\text{ml}^{-1}$).

177

178 **2.5. Analysis of cellular or extracellular character of IAA degradation**

179 *BjE109* was grown as described before, but 10 ml aliquots obtained from exponential
180 growth phase cultures were centrifuged at $12,000 \times g$ for 20 min (4°C). The
181 supernatants were used as control treatment for IAA degradation assays (extracellular
182 feature) as described before. The pellets were washed twice and resuspended in 10 ml of
183 20 mM Tris-HCl buffer pH 8.0 containing 1 mM EDTA, 10 mM MgCl_2 , 12.5 % (v/v)
184 glycerol, 0.1% (v/v) Triton, and the complete mini EDTA-free protease inhibitor
185 cocktail (Sigma-Aldrich, Germany). The cells were disrupted (lysed) by sonic treatment
186 (M.S.E. 150 W) for 210 s (in 30 s period), centrifuged and the cellular debris discarded.
187 The supernatants were used for IAA degradation assays (cellular feature).

188

189 **2.6 Evaluation of IAA degradation kinetics**

190 We assessed the kinetics of IAA degradation in both cell-free supernatants and
191 non-centrifuged cell cultures of *BjE109*.

192 In the case of cell cultures, we evaluated the addition of different concentrations of
193 exogenous IAA to *BjE109* cultures during exponential growth phase in order to estimate

194 the maximum quantity of IAA that this metabolically active microorganism is able to
195 degrade. To achieve this, cell cultures were incubated as previously described until early
196 exponential growth phase ($OD_{595} \approx 0.6$) and divided into 5 ml aliquots, which were added
197 into 10 ml sterile borosilicate tubes. After 15 min of stabilization at 30°C with orbital
198 shaking (180 rpm), 200 μ l of IAA solution or equivalent volume of sterilized water was
199 alternatively added into the tubes containing *BjE109* to obtain a final concentration ≈ 20 ,
200 40, 80, 120 and 160 μ g. ml^{-1} of IAA per tube. Control treatments using uninoculated YEM
201 medium modified by the addition of IAA solutions were also performed. Tubes were
202 incubated at 30°C with orbital shaking (180 rpm), and 500 μ l of the mixture was sampled
203 after 15 min (T_0), 8, 12, 24 and 32 h of incubation to measure IAA concentration
204 (μ g. ml^{-1}). The viability of *BjE109* cells was evaluated after 32 h of IAA addition by direct
205 plate counting on YEM agar, according to Vincent [21].

206 In the case of the cell-free supernatants, *BjE109* cultures were incubated at 30°C with
207 orbital shaking (180 rpm) until early exponential (EE) ($OD_{595} \approx 0.6$) or late exponential
208 (LE) ($OD_{595} \approx 1.2$) growth phase. A 50 ml aliquot obtained from these cultures was
209 centrifuged at 8000 rpm for 15 min, filtered (0.2 μ m) to obtain a cell free supernatant and
210 divided in 5 ml aliquot in borosilicate tubes for IAA-treatment as described before. The
211 treatments carried out were the following: (1) addition of pure IAA solution to EE
212 supernatant to obtain a final concentration ≈ 40 μ g. ml^{-1} IAA per tube; (2) addition of IAA
213 to LE supernatant to obtain a final concentration ≈ 40 μ g. ml^{-1} IAA per tube. Treatments
214 were performed in triplicate. Control treatments using uninoculated YEM medium
215 modified by the addition ≈ 40 μ g. ml^{-1} IAA solutions were also carried out. Tubes were
216 incubated as previously described, and 500 μ l of the mixture was sampled every 2 h to
217 measure IAA concentration (μ g. ml^{-1}).

218

219 **2.7 Analysis of IAA degradation pathway**

220 **2.7.1 Analysis *in silico***

221 Based on the canonical metabolic pathway described in *P. putida* 1290 by Leveau
222 and Gerards [10] for the IAA degradation, we analyzed the presence of similar proteins
223 by sequence comparison in the *BjE109* genome. For bioinformatics analysis, the
224 following tools (T) and databases were used: Blast (T) [24], KEGG [25], RAST [26],
225 T-coffee (T) [27], Smart [28], MaGe [29], UniProt [30] and InterPro [31].

226

227 **2.7.2 Construction of $\Delta iacC$ mutants**

228 The general cloning procedures were performed according to Sambrook et al. [32]
229 with minor modifications. The deletions in the *iacC* gene in both strains of
230 *Bradyrhizobium* were carried out through an unmarked in-frame deletion using the
231 pK18mobSacB plasmid carrying the counter-selection gene *sacB*, as described by
232 Mongiardini et al. [33]. Given the sequences similarity between the predicted *iacC* genes
233 (AJA64126.1 in E109 or blr3400 in USDA110), the PCR products were amplified with
234 the same set of primers, FW*iacCE* and RV*iacCH* (Table 1). The fragments were
235 gel-purified and cloned at the restriction sites *EcoRI/HindIII* into the pK18mobSacB [19]
236 giving the plasmids, pK18mobSacB::*iacCBd* and pK18mobSacB::*iacCBj* carrying the
237 *BdUSDA110* fragment and the *BjE109* fragment respectively. Each plasmid was *Sall*
238 digested which released a 468 bp fragment from the insert cloned before as exemplify for
239 *BjE109* in the Fig. S1. Then, each plasmid was re-ligated giving the final construction,
240 pK18mobSacB:: $\Delta iacCBd$ and pK18mobSacB:: $\Delta iacCBj$. These plasmids were
241 transferred by bi-parental conjugations to the corresponding wild-type strain according to
242 Quelas et al. [34] and simple-crossover transconjugants (cointegrate) were selected by
243 Km resistance in YEM media agar and the double crossover recombination was induced

244 by plating the transconjugants in YEM agar plates supplemented with 10% (w/v) sucrose.
245 These sucrose resistant clones, that resolve the recombinant plasmid and that are Km
246 sensitive, were checked by PCR to dissociate between the mutant and the wild-type
247 genotype. The mutants obtained carry an in-frame deletion in each *iacC* gene and were
248 named *BjE109 Δ iacC* and *BdUSDA110 Δ iacC*. All the plasmids and constructions are
249 listed in the Table 1.

250

251 **2.7.3 Restoration of the IAA degradation capacity in Δ iacC mutants**

252 The restored phenotype of the mutant *BjE109 Δ iacC* was obtained using competent
253 cells of *Escherichia coli* S-17 containing the pJN105 (pBBR) plasmid [20] with the *iacC*
254 cloned fragment inducible by L-arabinose. *E. coli* S-17 was grown in LB medium
255 modified by the addition of 30 $\mu\text{g}\cdot\text{ml}^{-1}$ gentamicin (Gm), and *BjE109* was grown in PSY
256 medium modified by the addition of L-arabinose [47]. For conjugation, *E. coli* S-17
257 culture was diluted a hundred times in LB medium without antibiotics and grown at 30°C
258 with orbital shaking (180 rpm) until $\text{OD}_{595}\approx 0.8-1$. Subsequently, a mix with 900 μl of
259 E109 culture during exponential growth phase with 400 μl of S-17 culture was made. The
260 culture mix was centrifuged for 8 minutes at 3000 rpm and the pellet was re-suspended
261 and placed in a plate containing PSY agar medium with L-arabinose. Plates were
262 incubated at 30°C for 48 h. Colonies were re-suspended and homogenized into 1 ml of
263 saline solution. A 150 μl aliquot of conjugation homogenate was placed in YEM medium
264 with 50 $\mu\text{g}\cdot\text{ml}^{-1}$ Gm and plates were incubated in the conditions previously mentioned for
265 72-96 h. The restored phenotype of *BjE109* named *BjE109 Δ iacC/pJN105iacC* was
266 evaluated in comparison with *BjE109* (wild type) and *BjE109 Δ iacC* as control
267 treatments.

268

269 **2.8 IAA biosynthesis and degradation in *BjE109*, *BdUSDA110* and their mutants**

270 We evaluated both degradation and biosynthesis of IAA by the *BjE109* and
271 *BdUSDA110* wild type strains and their mutants *BjE109ΔiacC*, *BdUSDA110ΔiacA* and
272 *BdUSDA110ΔiacC*. Cultures of each strain were incubated until early exponential
273 growth phase ($OD_{595} \approx 0.6$), and treated with IAA solution to obtain a final concentration \approx
274 $40 \mu\text{g}\cdot\text{ml}^{-1}$ IAA as described before. A control treatment using uninoculated YEM
275 medium, but modified by addition of pure IAA was also considered. Tubes were
276 incubated at 30°C with orbital shaking (180 rpm), and $500 \mu\text{l}$ of the mixture was taken
277 every 2 h incubation to measure IAA concentration ($\mu\text{g}\cdot\text{ml}^{-1}$). In the case of the IAA
278 biosynthesis, 250 ml flasks containing 100 ml of YEM culture medium modified by
279 addition of $10 \text{ mg}\cdot\text{l}^{-1}$ L-trp were inoculated with 10 % (v/v) *BjE109* cultures in early
280 exponential growth phase ($OD_{595} \approx 0.6$) or its mutant *BjE109ΔiacC*. Cultures were
281 incubated as previously described and after 12 h and 24 h of incubation samples were
282 taken to measure cell growth (OD_{595}) and IAA concentration ($\mu\text{g}\cdot\text{ml}^{-1}$).

283

284 **2.9 Identification of metabolites produced by IAA degradation**

285 The identification of IAA degradation metabolites was achieved by analyzing the
286 expression of the *BjE109* genes *iacC*, *iacD* or *iacCD* in the heterologous strain
287 *Cupriavidus pinatubonensis* JMP134 (Table 1) under the control of the AraBAD (P_{BAD})
288 promoter in the pBS1 plasmid [48]. This strain lacks *iac* gene sequences and is unable to
289 use IAA as a sole carbon and energy source which allow its use as an appropriate
290 heterologous host for higher expression of *iac* genes. An empty pBS1 plasmid (control)
291 and pBS1 derivatives containing *iacC*, *iacD* or *iacCD* were independently electroporated
292 in *C. pinatubonensis* JMP134 and selected in LB medium plus Gm ($30 \mu\text{g}\cdot\text{ml}^{-1}$). For the
293 expression of *iac* genes driven by the heterologous P_{BAD} promoter, these derivatives were

294 exposed to 5 mM L-arabinose [35]. Exponential growth cultures of *C. pinatubonensis*
295 JMP134 of 100 ml final volume were exposed to a final concentration of 40-160 $\mu\text{g}\cdot\text{ml}^{-1}$
296 IAA during 24 h and then analyzed for metabolites identification. The organic fraction of
297 the culture medium was extracted by triplicate using an equal volume of ethyl acetate.
298 Then, the organic layer was dried over anhydrous Na_2SO_4 and filtered, and the solvent
299 was removed in vacuum. The resultant mixture of products was subjected to a
300 spectroscopic analysis. The NMR (nuclear magnetic resonance) spectra were recorded on
301 a Bruker Advance III HD 400 at 400 MHz for ^1H and 100 MHz for ^{13}C . NMR spectra
302 were recorded in $\text{DMSO-}d_6$ (dimethyl sulfoxide), using the solvent signal as reference.
303 The chemical shifts are expressed in ppm (δ scale) downfield from tetramethylsilane
304 (TMS) and coupling constant values (J) are given in Hertz. The mass spectra were
305 determined in TQ 4500 triple-quadrupole mass spectrometer coupled with electrospray
306 ionization (ESI) source and were operated in the negative ion mode. The IAA degradation
307 metabolites identified by expression of *iac* genes in *C. pinatubonensis* JMP134 were
308 evaluated by spectroscopic and spectrometric analysis in late exponential cultures of
309 *BjE109* obtained from YEM culture media exposed during 24 h to $\approx 40 \mu\text{g}\cdot\text{ml}^{-1}$ IAA. The
310 analytical procedure was the same previously described.

311

312 **2.10 *Bradyrhizobium*-soybean symbiosis in *BjE109*, *BdUSDA110* and their mutants**

313 Cultures of *BjE109*, *BdUSDA110* and *iacC* mutants, grown as previously described
314 in section 2.1, were used to inoculate soybean seeds cv. Don Mario 4800 with a $3 \text{ ml}\cdot\text{kg}^{-1}$
315 dose (Note: this dose is normally used under field conditions by most of the agricultural
316 companies). The nodulation pattern was individually evaluated on both inoculated and
317 non-inoculated (control) seeds according to Burton et al. [36] with some modifications.

318 A triplicate of 9 soybean seeds (n=27) were sown in three separate plastic pots (300 ml
319 volume capacity) containing vermiculite as a solid substrate, irrigated with
320 nitrogen-deficient sterile N-free Hoagland's solution (25% v/v) [37]. The seedlings were
321 maintained for 21 days in a growth chamber at 30/20 °C and 80% relative humidity with
322 a 16/8 h day/night photoperiod. At the end of the experiment, the following parameters
323 were measured: (1) number of nodules on the main root per plant, (2) number of nodules
324 on the secondary roots per plant, (3) number of nodules per plant, following Burton et al.
325 [36], and (4) shoot and root dry weight.

326

327 **2.11 Statistical analyses**

328 Treatments were performed in triplicate from three independent experiments. Values
329 shown represent mean \pm standard deviation (SD). Results of IAA degradation were
330 analyzed by the Kruskal-Wallis non-parametric test, while results obtained from soybean
331 symbiosis assays were analyzed by ANOVA followed by a Tukey's *post hoc* analysis at
332 $p < 0.05$. Analyses and graphs were performed using the PRISM V 4.0 statistical package
333 for Windows (GraphPad Software, San Diego, CA USA).

334

335 **3. Results**

336 **3.1 IAA degradation by *Bradyrhizobium***

337 We measured the evolution of IAA concentration ($\mu\text{g}\cdot\text{ml}^{-1}$) along time in
338 exponential cultures of *BjE109*, *BdUSDA110* and *BeSEMIA5019* modified by the
339 exogenous addition of the hormone.

340

341 **Fig. 1**

342

343 The concentration of IAA in cultures of *BjE109* and *BdUSDA110*, modified by the
344 addition of the hormone, decreased as a function of time (Fig. 1A). A 50% decrease of
345 in the IAA concentration was observed 8 h after addition, whereas it was no longer
346 detected in culture media after 24 h of incubation. Despite both *BjE109* and
347 *BdUSDA110* strains were able at 24 h after addition to degrade all the IAA, the
348 degradation rate in *BdUSDA110* ($6.570 \pm 0.2754 \mu\text{g}\cdot\text{ml}^{-1}\cdot\text{h}^{-1}$) was faster than *BjE109*
349 ($5.655 \pm 0.4524 \mu\text{g}\cdot\text{ml}^{-1}\cdot\text{h}^{-1}$) between 4 and 8 h after addition. On the other hand,
350 *BeSEMIA5019* was unable to degrade IAA and the hormone concentration was
351 maintained along the experiment and even found to be slightly increased after 24 h of
352 incubation, presumably as a result of the ability of this bacterium to synthesize this
353 molecule [15]. In the case of uninoculated YEM culture media, the IAA concentration
354 ($\mu\text{g}\cdot\text{ml}^{-1}$) did not change over time, probably because the culture medium did not affect
355 the stability of the molecule.

356 To elucidate the nature of the molecule responsible for IAA degradation in *BjE109*,
357 we measured the IAA concentration ($\mu\text{g}\cdot\text{ml}^{-1}$) in supernatants (sE109) and heat
358 denatured supernatants (sE109 ϕ). For that, around $40 \mu\text{g}\cdot\text{ml}^{-1}$ IAA was added to each
359 treatment. A significant decrease in the IAA concentration ($\mu\text{g}\cdot\text{ml}^{-1}$) was observed 4 h
360 after addition of the hormone in sE109, while a complete absence of the molecule was

361 found after 8 h of incubation (Fig.1B). IAA concentration in sE109 ϕ did not change
362 over time. No IAA degradation was observed in disrupted cells (lysates cells) indicating
363 the extracellular feature of the activity. Under our experimental conditions, results
364 suggest the molecule responsible for IAA degradation should be released into the
365 culture medium (extracellular feature) before IAA addition (constitutive feature). The
366 loss of activity in the supernatants following heat denaturation suggested an enzyme
367 candidate.

368

369 **3.2 Evaluation of the kinetics for IAA degradation by BjE109**

370 We evaluated the IAA degradation kinetics of BjE109 by the use of two different
371 approaches. In the first one, we estimated the maximum concentration of IAA that could
372 be degraded by these bacteria, using the whole exponential cultures of BjE109. Results
373 of these experiments are summarized in Fig. 2. In the second approach, we used the
374 supernatants obtained from both early (EE) and late exponential (LE) growth phases of
375 BjE109 cultures and these results are summarized in Fig.3.

376

377 **Fig.2**

378

379 Fig.2 shows that BjE109 cultures under exponential growth phase were able to fully
380 degrade up to $\approx 80 \mu\text{g}\cdot\text{ml}^{-1}$ of exogenous IAA after 24 h of treatment. However, at
381 higher concentrations of the hormone (i.e. around 120 and 160 $\mu\text{g}\cdot\text{ml}^{-1}$), there was a

382 reduction in the degradation capacity: about 50% of the initial concentration was
383 measured at the end of the experiment, clearly showing a saturation kinetics after 8 h of
384 IAA treatment over $80 \mu\text{g}\cdot\text{ml}^{-1}$. The viability of the *BjE109* was measured at 24, 36 and
385 48 h incubation by direct plate counting on YEM agar and no significant variations
386 between treatments were recorded.

387

388 **Fig.3**

389

390 Fig.3 shows that supernatants of *BjE109* cultures obtained from both early (EE) and
391 late exponential (LE) growth phases had different kinetics for IAA degradation after 12
392 h of IAA treatment. The supernatants obtained from the late exponential (LE) growth
393 phase of *BjE109* cultures degrade the IAA more rapidly than the ones obtained from the
394 early exponential (EE) growth phase. This behavior is probably due to the fact that
395 enzyme biosynthesis has kinetics similar to that of a primary metabolite produced
396 during bacterial growth, in which the accumulation of the enzyme into the culture
397 medium increases the degradation capacity of IAA per unit of time.

398

399 **3.3. IAA degradation is encoded in the genome of *B. japonicumE109***

400 Based on the metabolic pathway described in *P. putida* 1290 by Leveau and
401 Gerards [10] for the IAA degradation, we checked for the presence of similar sequences
402 in the *BjE109* genome. The results of the *in silico* analyses are showed in Table S1. We

403 found homologous sequences for all the proteins related to the *iac* cluster of *P. putida*
404 1290 in the *BjE109* genome; however, they are not located in a unique cluster of genes
405 but distributed along the genome in a random way. The protein sequence with highest
406 amino acid similarity is the one homologue to *iacA*, which codes for an acyl-CoA
407 dehydrogenase in *BjE109*. The protein encoded by the *iacA* gene has been previously
408 reported in *BdUSDA110* as NrgC, which is regulated by NifA during the
409 *Bradyrhizobium*-soybean interaction [16]. We assessed the IAA degradation by
410 *BdUSDA110ΔiacA* mutant [16] and fully discarded that *iacA* expression product would
411 participate in the IAA degradation process (Fig. 4).

412

413 **Fig. 4.**

414

415 The wild type strain degraded 100% of the 40 $\mu\text{g}\cdot\text{ml}^{-1}$ IAA added in the culture
416 medium before 24 h of incubation. This behavior was similar to that of the mutant
417 *BdUSDA110ΔiacA*. In our experimental conditions the gene *iacA* was not involved in
418 IAA catabolism, thus this result allowed us to abandon the hypothesis about *iacA* as the
419 main responsible for IAA degradation. In the case of the $\Delta iacC$, the results showed that
420 the mutant strain could not degrade the hormone and this fact indicates that the product
421 of *iacC* is required for IAA degradation in *BdUSDA110*.

422

423 **3.3.1 The *iacCDF* cluster of *BjE109***

424 The *in silico* analysis of the *BjE109* genome shows that *iacC* codes for an
425 oxidoreductase 3-phenylpropionate dioxygenase (α -subunit), according to the Blast-p
426 tool of NCBI and RAST database (Fig. S2). The *iacC* is flanked by *iacD*, which codes
427 for a 3-phenylpropionate dioxygenase (β -subunit) and *iacF*, which codes for a
428 ferredoxin and grouped with two additional genes encoding for long chain fatty acid
429 CoA ligase and an oxidoreductase, forming a separate cluster in the genome of *BjE109*
430 (Fig. S2). We performed a complementary analysis of the *IacC* sequence by SignalP-5.0
431 (<http://www.cbs.dtu.dk/services/SignalP/>) and established its tentative extracellular
432 localization by the presence of a TAT [Tat/SP] signal peptide, responsible for the
433 protein translocation. Finally, the *iacC* sequence of *BjE109* was compared with similar
434 sequences obtained from other strains belonging to different species of the genus
435 *Bradyrhizobium*. In the case of those strains belonging to the same species as *BjE109*, the
436 *iacC* gene identity was higher than 97%, while in other species the identity decreased by
437 95-91% (Table S2) with *B. yuanmingense* and *B. diazoefficiens* as the closest to *B.*
438 *japonicum*.

439

440 **3.4 IAA degradation by *B. japonicum* E109 and E109 Δ *iacC* mutant**

441 Taking into account the *in silico* analysis, we decided to consider the *iacC* of
442 *BjE109* as the target gene for mutagenesis procedure. The main objective of this
443 procedure was to obtain the *BjE109 Δ *iacC** mutant and to evaluate the capacity of such
444 strain to degrade IAA in comparison with the wild type one.

445

446 **Fig.5.**

447

448 Fig.5 shows that *BjE109ΔiacC* mutant was unable to degrade IAA when the
449 molecule was exogenously added into the culture medium, even for a long period of 48
450 h incubation. On the contrary, the strain *BjE109* degraded 100% of the $\approx 40 \mu\text{g.ml}^{-1}$
451 IAA in the culture medium before 24 h of incubation. To confirm that the observed
452 phenotype was due to the mutation in the *iacC*, we evaluated the complemented strain
453 *BjE109ΔiacC/pJN105iacC*. The capacity to degrade IAA was resumed: after IAA
454 addition a 28% IAA degradation ($10.96 \mu\text{g.ml}^{-1}$) in the first 24 h, a 72% after 48 h (28.4
455 $\mu\text{g.ml}^{-1}$) and a 90% after 72 h ($34.1 \mu\text{g.ml}^{-1}$) was measured (Fig. 5). On the other hand,
456 the IAA concentration did not change along the experiment ($\approx 40 \mu\text{g.ml}^{-1}$) in the case of
457 the *BjE109ΔiacC* mutant, in contrast to the *BjE109* strain, for which IAA degradation
458 was 100% at 24 h after IAA-treatment. These results allowed us to confirm that *iacC*
459 codes for the putative enzyme responsible for IAA degradation in this bacterium.
460 Experiments of heterologous expression in *C. pinatubonensis* JMP134 showed that the
461 product of *iacD* alone and the control with empty vector were not able to degrade ≈ 40
462 $\mu\text{g.ml}^{-1}$ IAA in comparison with the product of *iacC* and *iacCD* genes, which were able
463 to degrade this molecule in less than 24 h incubation.

464

465 **3.5 Evaluation of IAA biosynthesis in the *BjE109ΔiacC***

466 In a previous report using liquid chromatography-multiple reaction
467 monitoring-mass spectrometry (LC-MRM-MS), we found a negligible amount of IAA
468 ($0.67 \text{ pmol.ml}^{-1}$) in supernatants of *BjE109*. However, the molecule did not accumulate
469 into the culture medium at a significant concentration to be detected by HPLC, we thus
470 concluded that this strain was unable to produce IAA [15]. In this study, no significant
471 amount of IAA was detected by HPLC for both wild type and the mutant *BjE109 Δ iacC*.
472 The mutation in the *iacC* gene led to the bacterium losing the ability to degrade IAA;
473 however, the mutant did not release a detectable amount of the hormone in the culture
474 media. The results obtained in this paper (under defined experimental conditions), in
475 addition to those previously published [15] and our particular experience modifying a
476 broad range of experimental conditions (i.e. culture media, incubation time,
477 temperature, etc.) to evaluate the bacterial capacity to biosynthesize IAA (data not
478 shown), allow us to conclude that the *BjE109* has no significant activity in any of the
479 proposed pathways for IAA biosynthesis and thus it cannot synthesize it in significant
480 amounts.

481

482 **3.6 Metabolites of IAA catabolism in *BjE109***

483 The metabolites deriving from the *iacCD* expression in *C. pinatubonensis* JMP134
484 in presence of IAA were analyzed by different spectroscopic and spectrometric
485 techniques ($^1\text{H-NMR}$, $^{13}\text{C-NMR}$, DEPT, MS) (Fig. S3, S4 and S5) and confirmed in
486 *BjE109* cultures modified by the presence of the hormone. The $^1\text{H-NMR}$ spectrum

487 analyses indicated that the product of degradation of IAA contained two metabolites in
488 equal proportions with a structural similarity. Chemically, both metabolites showed an
489 intact phenyl ring and a signal concordant with CH group between 5-6 ppm. This result
490 suggests that the pyrrole ring of the IAA molecule was saturated at positions C2-C3. On
491 the other hand, the presence of signals corresponding to aliphatic hydrogen atoms
492 between 2-3 ppm indicates that a methylene group adjacent to the carboxylic group
493 presents both hydrogens with a different magnetic environment, suggesting that the
494 pyrrole ring was modified in both metabolites in relation to the precursor IAA. The
495 ^{13}C -NMR spectrum analysis indicated that both metabolites have a carbonyl group with
496 a similar magnetic environment, reinforcing the idea that both products have very
497 similar identities. Also, the joint analysis of the ^{13}C -NMR and DEPT spectra indicated
498 the presence of one carbonyl group, three quaternary carbon atoms, five CH groups and
499 one methylene group for each of the molecules. The number and type of carbon atoms
500 finding in metabolites are equal to the presents in the precursor (IAA); however, the
501 displacement of one of the CH groups and of one of the quaternary carbons accounts for
502 an aliphatic rather than aromatic character for these two carbon atoms. The MS analysis
503 indicated the presence of two compounds with a mass of 190.8 (A) and 224.9 (C)
504 $\text{g}\cdot\text{mol}^{-1}$, respectively (Fig S3, S4, S5 and Fig. 6). The IAA molecule has an exact mass
505 of 175.1 $\text{g}\cdot\text{mol}^{-1}$. Mass difference of 190.8 $\text{g}\cdot\text{mol}^{-1}$ between IAA and the metabolite A is
506 equal to the mass of an oxygen atom. This experimental data together with NMR
507 evidences allow us to postulate that the molecule A is one of the metabolites isolated

508 from IAA degradation by E109. However, the presence of the metabolite C (224.9
509 g.mol⁻¹) in the degradation product was interesting, as from a chemical point of view the
510 logical sequence would be the opening of the epoxide group in A by a molecule of
511 water to obtain the molecule B (209.7 g.mol⁻¹). Nevertheless, MS did not show any
512 compound B with a 209 g.mol⁻¹. Summarizing, analyses by ¹H and ¹³C NMR
513 spectroscopy and mass spectrometry suggested that purified compounds produced by
514 IAA degradation in *BjE109* are 3-indoleacetic acid 2,3-oxide or
515 2-(1a,2-dihydro-6bH-oxireno [2,3-b] indol-6b-yl) acetic acid, according to IUPAC (A)
516 and 2-(2-hydroperoxy-3-hydroxyindolin-3-yl) acetic acid (C).

517

518 **Fig.6.**

519

520 **3.7 *Bradyrhizobium*-soybean symbiosis in *BjE109*, *BdUSDA110* and their mutants**

521 Table 2 shows the growth and nodulation of soybean seedlings inoculated with
522 *BjE109*, *BdUSDA110* and their *iacC* mutants.

523

524 **Table 2**

525

526 Plant growth and nodulation increased in soybean plants obtained from inoculated
527 seeds as compared to those uninoculated, in which no nodule was observed. In the case
528 of inoculated seeds, nodulation as MRN (main root nodules), SRN (secondary root

529 nodules) and RN (root nodules) increased in plants treated with the wild type strain in
530 comparison with *iacC* mutants. The MRN, SRN and RN of *BjE109* inoculated plants
531 increased by 25.6, 16.4 and 21.6% respectively, in comparison with *BjE109ΔiacC*. In
532 the case of *BdUSDA110*, plants inoculated with this strain increased by 42.8; 35.0 and
533 40.4% respectively in comparison with the mutant. Shoot dry weight increased by
534 18.0% and 20.6% in plants inoculated with *BjE109* and *BdUSDA110* respectively, in
535 comparison with the ones inoculated with the *iacC* mutants. Root dry weight increased
536 by 21.9% and 8.7% in plants inoculated with wild type strains in comparison with
537 mutants.

538

539 **4. Discussion**

540 Minamisawa and Fukai [38] observed, for the first time, that some strains of *B.*
541 *japonicum* were unable to accumulate IAA in the culture media. They suggested that
542 such strains were unable to produce IAA or degraded the molecule after its biosynthesis.
543 At the same time, Egebo et al. [8] confirmed that *BdUSDA110* degraded IAA under an
544 oxygen-dependent reaction and suggested that IAA is oxidized to aminobenzoyl-acetic
545 acid and anthranilic acid by a putative tryptophan 2,3-dioxygenase. A different pathway
546 for IAA degradation, starting with an oxidation of IAA to anthranilic acid, was proposed
547 by Jensen et al. [9]. They reported the production of dioxindole-3-acetic acid,
548 dioxindole, isatin, 2-aminophenyl glyoxylic acid (isatinic acid) and anthranilic acid as
549 metabolites related to IAA catabolism in *BdUSDA110*. Olesen and Jochimsen [39]

550 suggested that both an isatin reductase and isatin amidohydrolase were responsible of
551 IAA degradation in *B. japonicum*. However, these metabolites or the related enzymes
552 were not identified in this or later reports [40]. A transcriptional analysis of
553 *BdUSDA110* after exogenous treatment with 1 mM of IAA did not reveal a potential
554 catabolic pathway of IAA or any enzymes involved [41]. Recently, we confirmed the
555 non-assimilative degradation of both natural and synthetic auxins in *BjE109* cultures
556 after 24 h exposition [15]. In the present work we showed two new features about the
557 IAA degradation in *BjE109*. The IAA degradation capacity is preexisting to the
558 exogenous addition of the molecule in the culture medium and the degradation capacity
559 occurs in the extracellular environment. The denaturation by heat of *BjE109*
560 supernatants led to the complete loss of IAA degradation capacity, supporting the
561 existence of a preexisting (constitutive) and extracellular enzyme as responsible.

562 Two different clusters for IAA catabolism have been characterized in eubacteria,
563 the *iac* cluster identified in the alphaproteobacteria *P. putida* 1290 [10] and the *iaa*
564 cluster identified in the betaproteobacteria *A. aromaticum* EbN1 [11]. In the case of *P.*
565 *putida* 1290, which uses IAA as a sole source of carbon and energy, it contains a cluster
566 of 10 genes [10]. The canonical cluster of *P. putida* 1290 is well conserved and named
567 the *iac*ABCDEFGRHI gene cluster. The *iacA* encodes the acyl-CoA dehydrogenase,
568 which would start the IAA degradation attacking the indole ring of IAA, thus generating
569 2-hydroxy-IAA. The *iacB* encodes a conserved hypothetical protein with unknown
570 functions. The *iacC* and *iacD* genes encode the alpha and beta subunits of Rieske (2Fe–

571 2S) domain containing aromatic ring hydroxylating dioxygenase, which is involved in
572 3-hydroxy-2-oxo-IAA conversion to catechol. The *iacE* encodes a short-chain
573 dehydrogenase/reductase, which is involved in the conversion of 2-hydroxy-IAA to
574 3-hydroxy-2-oxo-IAA. The *iacF* encodes for ferredoxin and the *iacG* encodes a flavin
575 reductase domain protein. This protein, in *P. phytofirmans* PsJN, might provide reduced
576 flavins to the IacA protein [35]. The *iacH* and *iacI* genes, which encode for a putative
577 Glu-tRNA amidotransferase and conserved hypothetical protein respectively, both have
578 unknown functions. The *iacR* encodes for transcriptional regulator of the MarR family
579 [42-43]. *P. putida* 1290 carries two copies each of the *iacC*, *iacD* and *iacF* genes [44]. In
580 the case of *BjE109*, the *iacC* gene forms a separate cluster together with *iacD*, *iacF* and
581 two additional genes (Fig. S2). Based on this fact, we constructed the *BjE109ΔiacC*
582 mutant and observed the full loss of IAA degradation capacity We then confirm the role
583 of 3-phenylpropionate dioxygenase (α -subunit) in the IAA degradation process.

584 Both, *P. putida* 1290 and *Caballeronia glathei* DSM 50014 utilize IAA as a sole
585 source of carbon and energy and the final product of this pathway is catechol [10;45].
586 The first reaction is catalyzed by IacA, which converts IAA to 2-hydroxy-IAA
587 (2-oxindole-3-acetic acid) [42] or 2,3-dihydroxy-indoline-3-acetic acid, according to
588 Sadauskas et al. [45]. Then, IacE catalyzes the conversion of these metabolites to
589 3-hydroxy-2-oxindole-3-acetic acid (dioxindole-3-acetic acid). The conversion of
590 dioxindole-3-acetic acid to the final product, catechol, involves multiple reactions but
591 mainly are carried out by IacC and IacD. Both *BjE109* cultures and heterologous

592 expression of *iacC* or *iacCD* genes in *C. pinatubonensis* JMP134 during IAA
593 degradation allowed us to identify 3-indoleacetic acid 2,3-oxide and
594 2-(2-hydroperoxy-3-hydroxyindolin-3-yl) acetic acid. These metabolites were not
595 produced in any of the pathways previously described in both *BdUSDA110* and *P.*
596 *putida* 1290.

597 *Bradyrhizobium* sp. has been extensively studied because of its symbiotic
598 association with legumes and its biological nitrogen fixation capacity. *BjE109* is broadly
599 used to inoculate soybean seeds because it has the ability to increase the performance of
600 the legumes under agronomic conditions [46]. In a previous report, we observed that
601 addition of IAA to *BjE109* cultures increased the viable cell recovery from soybean
602 seeds after inoculation, in comparison with the untreated control [15]. In similar
603 experiments, Donati et al. [41] examined the effect of pretreatment with IAA on the
604 ability of *BdUSDA110* to nodulate soybean roots, but in this report, none of the
605 pretreatments affected the number of nodules, nodule weight, or plant weight. In our
606 experiments *BjE109* and *BdUSDA110* were able to increase the number of nodules and
607 dry weight of shoots and roots in soybean plants in comparison with the mutants *iacC*,
608 unable to degrade the phytohormone. These parameters were remarkably higher in
609 *BdUSDA110* in comparison to plants inoculated with *BjE109*. Summarizing, the
610 inability of the *iacC* mutants to degrade the hormone determined a change in their
611 symbiotic behavior: the establishment of the symbiosis at the level of the nodules
612 number and their location in the roots, as well as the growth of the inoculated plant, were

613 negatively affected. This behavior could be partially due to the change in the mutant's
614 abilities related to: (a) the survival on soybean seeds after inoculation; (b) the
615 colonization of roots after germination or (c) the formation of active nodules during
616 symbiosis process. This issue should be addressed in a future work.

617 In this study, we have presented new molecular and physiological evidences related
618 to the IAA degradation in *B. japonicum* and we have proposed a putative model/pathway
619 for IAA degradation in this bacterium.

620

621 **Conflicts of Interest**

622 The authors declare no conflict of interest

623

624 **Acknowledgments**

625 We thank to Instituto de Investigaciones Agrobiotecnológicas (INIAB); Universidad
626 Nacional de Río Cuarto (UNRC); Consejo Nacional de Investigaciones Científicas y
627 Tecnológicas (CONICET), Fondo Nacional de Ciencia y Tecnología (FONCyT);
628 Instituto de Biotecnología y Biología Molecular (IBBM); Pontificia Universidad Católica
629 de Chile (PUC); Fondo de Equipamiento Científico y Tecnológico (FONDEQUIP),
630 project EQM120021. R.D. acknowledges support by ANID PIA/Anillo ACT172128 and
631 ANID PIA/BASAL FB0002 grants. FC is Researcher of CONICET at the UNRC. DT is a
632 Postdoctoral researcher at the UNRC granted by CONICET. JG and FD are PhD student
633 at the UNRC granted by CONICET. We would like to thank Coline Le Noir de Carlan for
634 her contribution in the English revision of this manuscript.

635

636 **References**

- 637 1. Glick BR, Patten C, Holguin G, Penrose D. Auxin production. *In* Biochemical and
638 genetic mechanisms used by plant growth promoting bacteria, Imperial College
639 Press, London, England, 1999, p 86-133.
- 640 2. Sekine M, Ichikawa T, Kuga N, Kobayashi M, Sakurai A, Syōno K. Detection of
641 the IAA biosynthetic pathway from tryptophan via indole-3-acetamide in
642 *Bradyrhizobium* spp. *Plant Cell Physiol* 1988; 29(5):867-874.
643 <https://doi.org/10.1093/oxfordjournals.pcp.a077574>
- 644 3. Sekine M, Watanabe K, Syōno K. Molecular cloning of a gene for
645 indole-3-acetamide hydrolase from *Bradyrhizobium japonicum*. *J Bacteriol* 1989;
646 171(3):1718-1724. <https://doi.org/10.1128/jb.171.3.1718-1724.1989>
- 647 4. Kaneshiro T, Kwolek WF. Stimulated nodulation of soybeans by *Rhizobium*
648 *japonicum* mutant (B-14075) that catabolizes the conversion of tryptophan to
649 indol-3-yl-acetic acid. *Plant Sci* 1985; 42(3):141-146.
650 [https://doi.org/10.1016/0168-9452\(85\)90119-0](https://doi.org/10.1016/0168-9452(85)90119-0)
- 651 5. Thimann KV. On the physiology of the formation of nodules on legume roots. *Proc*
652 *Natl Acad Sci USA* 1936; 22(8):511-514. <https://doi.org/10.1073/pnas.22.8.511>
- 653 6. Taller B, Sturtevant D. Modification of cytokinin production in *Bradyrhizobium*
654 cultures. *J Cell Biochem Suppl* 1989; 12(Part C) 274.

- 655 7. Nielsen SV, Egebo LA, Jochimsen B. *Bradyrhizobial* indoleacetic acid metabolism
656 and its significance for root nodule development. *In* Molecular Genetics of
657 Plant-Microbe Interactions APS Press St Paul MN, 1988, 151-152.
- 658 8. Egebo LA, Nielsen SV, Jochimsen BU. Oxygen-dependent catabolism of
659 indole-3-acetic acid in *Bradyrhizobium japonicum*. *J Bacteriol* 1991; 173(15):
660 4897-4901. <https://doi.org/10.1128/jb.173.15.4897-4901.1991>
- 661 9. Jensen JB, Egsgaard H, Van Onckelen H, Jochimsen BU. Catabolism of
662 indole-3-acetic acid and 4- and 5-chloroindole-3-acetic acid in *Bradyrhizobium*
663 *japonicum*. *J Bacteriol* 1995; 177(20):5762-5766.
664 <https://doi.org/10.1128/jb.177.20.5762-5766.1995>
- 665 10. Leveau JH, Gerards S. Discovery of a bacterial gene cluster for catabolism of the
666 plant hormone indole 3-acetic acid. *FEMS MicrobiolEcol* 2008; 65(2):238-250.
667 <https://doi.org/10.1111/j.1574-6941.2008.00436.x>
- 668 11. Ebenau-Jehle C, Thomas M, Scharf G, Kockelkorn D, Knapp B, Schühle K, et al.
669 Anaerobic metabolism of indoleacetate. *J Bacteriol* 2012; 194:2894–2903.
670 <https://doi.org/10.1128/JB.00250-12>
- 671 12. Piccinetti C, Arias N, Ventimiglia L, Díaz Zorita M, Murua L, Sánchez H, et al.
672 Positive effects of inoculation of soybean on nodulation BNF and the parameters of
673 crop production. *In* Microbiología agrícola: un aporte de la investigación en
674 Argentina, 2nd ed, Albanesi AS (ed) Magna Publicaciones, Tucumán, Argentina,
675 2013, 283–297.

- 676 13. Torres D, Revale S, Obando M, Maroniche G, Paris G, Peticari A, et al. Genome
677 sequence of *Bradyrhizobium japonicum* E109, one of the most agronomically used
678 nitrogen-fixing rhizobacteria in Argentina. *Genome Announc* 2015;
679 3(1):e01566-14. <https://doi.org/10.1128/genomeA.01566-14>
- 680 14. Costacurta A, Vanderleyden J. Synthesis of phytohormones by plant-associated
681 bacteria. *Crit rev microbiol* 1995; 21(1):1-18.
682 <https://doi.org/10.3109/10408419509113531>
- 683 15. Torres D, Benavidez I, Donadío F, Mongiardini E, Rosas S, Spaepen S, et al. New
684 insights into auxin metabolism in *Bradyrhizobium japonicum*. *Res microbial* 2018;
685 169(6):313-323. <https://doi.org/10.1016/j.resmic.2018.04.002>
- 686 16. Nienaber A, Huber A, Göttfert M, Hennecke H, Fischer H. Three new
687 NifA-regulated genes in the *Bradyrhizobium japonicum* symbiotic gene region
688 discovered by competitive DNA-RNA hybridization. *J Bacteriol* 2000;
689 82(6):1472-1480. <https://doi.org/10.1128/JB.182.6.1472-1480.2000>
- 690 17. Alemayehu D, Gordon LM, O'Mahony MM, O'Leary ND, Dobson ADW. Cloning
691 and functional analysis by gene disruption of a novel gene involved in indigo
692 production and fluoranthene metabolism in *Pseudomonas alcaligenes* PA-10.
693 *FEMS Microbiol Lett* 2004; 239(2):285-293.
694 <https://doi.org/10.1016/j.femsle.2004.08.046>
- 695 18. Kaneko T, Nakamura Y, Sato S, Minamisawa K, Uchiumi T, Sasamoto S, et al.
696 Complete genomic sequence of nitrogen-fixing symbiotic bacterium

- 697 *Bradyrhizobium japonicum* USDA110. DNA Res 2002; 9(6):189-197.
698 <https://doi.org/10.1093/dnares/9.6.189>
- 699 19. Schäfer A, Tauch A, Jäger W, Kalinowski J, Thierbach G, Pühler A. Small
700 mobilizable multi-purpose cloning vectors derived from the *Escherichia coli*
701 plasmids pK18 and pK19: selection of defined deletions in the chromosome of
702 *Corynebacterium glutamicum*. Gene 1994; 145 (1):69–73.
703 [https://doi.org/10.1016/0378-1119\(94\)90324-7](https://doi.org/10.1016/0378-1119(94)90324-7) ANTES 30
- 704 20. Newman JR, Fuqua C. Broad-host-range expression vectors that carry the
705 L-arabinose-inducible *Escherichia coli* araBAD promoter and the araC regulator.
706 Gene 1999; 227(2):197-203. [https://doi.org/10.1016/S0378-1119\(98\)00601-5](https://doi.org/10.1016/S0378-1119(98)00601-5)
- 707 21. Vincent JA. 1970. Manual for the Practical Study of Root-nodul Bacteria. Int Biol
708 Program Handb, Blackwell, Oxford. <https://doi.org/10.1093/nar/gki106>
- 709 22. Cassán F, Vanderleyden J, Spaepen S. Physiological and agronomical aspects of
710 phytohormone production by model plant-growth-promoting rhizobacteria (PGPR)
711 belonging to the genus *Azospirillum*. J Plant Growth Regul 2014; 33(2):440-459.
712 <https://doi.org/10.1007/s00344-013-9362-4>
- 713 23. Glickmann E, Dessaux Y. A critical examination of the specificity of the salkowski
714 reagent for indolic compounds produced by phytopathogenic bacteria. Appl
715 Environ Microbiol 1995; 61(2):793-796.
716 <https://doi.org/10.1128/AEM.61.2.793-796.1995>

- 717 24. Madden T, Busby B, Ye J. Reply to the paper: Misunderstood parameters of NCBI
718 BLAST impacts the correctness of bioinformatics workflows. *Bioinformatics* 2019;
719 35(15):2699-2700. <https://doi.org/10.1093/bioinformatics/bty1026>
- 720 25. Kanehisa M, Goto S, Sato Y, Furumichi M, Tanabe M. KEGG for integration and
721 interpretation of large-scale molecular data sets. *Nucleic Acids Res* 2012;
722 40(D1):109-114. <https://doi.org/10.1093/nar/gkr988>
- 723 26. Aziz RK, Bartels D, Best AA, DeJongh M, Disz T, Edwards RA, et al. The RAST
724 Server: rapid annotations using subsystems technology. *BMC Genom* 2008;
725 9(1):75. <https://doi.org/10.1186/1471-2164-9-75>
- 726 27. Notredame C, Higgins D, Heringa J. T-Coffee: A novel method for fast and
727 accurate multiple sequence alignment. *J Mol Biol* 2000; 302(1):205-217.
728 <https://doi.org/10.1006/jmbi.2000.4042>
- 729 28. Letunic I, Bork P. 20 years of the SMART protein domain annotation resource.
730 *Nucleic Acids Res* 2018; 46(1):493-496. <https://doi.org/10.1093/nar/gkx922>
- 731 29. Vallenet D, Labarre L, Rouy Z, Barbe V, Bocs S, Cruveiller S, et al. MaGe: a
732 microbial genome annotation system supported by synteny results. *Nucleic Acids*
733 *Res* 2006; 34(1):53-65. <https://doi.org/10.1093/nar/gkj406>
- 734 30. Apweiler R, Bairoch A, Wu CH, Barker WC, Boeckmann B, Ferro S, et al.
735 UniProt: the universal protein knowledgebase. *Nucleic Acids Res* 2004;
736 32(1):115-119. <https://doi.org/10.1093/nar/gkh131>

- 737 31. Mulder N, Apweiler R, Attwood T, Bairoch A, Bateman A, Binns D, et al.
738 InterPro, progress and status in 2005. *Nucleic Acids Res* 2005; 33(1):201-205.
739 <https://doi.org/10.1093/nar/gki106>
- 740 32. Sambrook J, Fritsch E, Maniatis T. *Molecular cloning: a laboratory manual*, ed 2,
741 Cold Spring Harbor Laboratory Press: Cold Spring Harbor, NY, USA, 1989.
- 742 33. Mongiardini E, Quelas J, Dardis C, Althabegoiti M, Lodeiro A. Transcriptional
743 control of the lateral-flagellar genes of *Bradyrhizobium diazoefficiens*. *J Bacteriol*
744 2017; 199(15): e00253-17. <https://doi.org/10.1128/JB.00253-17>
- 745 34. Quelas JI, Mongiardini EJ, Casabuono A, López-García SL, Althabegoiti MJ,
746 Covelli JM, et al. Lack of galactose or galacturonic acid in *Bradyrhizobium*
747 *japonicum* USDA110 exopolysaccharide leads to different symbiotic responses in
748 soybean. *Mol Plant-Microbe Interact* 2010; 23(12):1592-1604.
749 <https://doi.org/10.1094/MPMI-05-10-0122>
- 750 35. Donoso R, Leiva-Novoa P, Zúñiga A, Timmermann T, Recabarren-Gajardo G,
751 González B. Biochemical and genetic bases of indole-3-acetic acid (auxin
752 phytohormone) degradation by the plant-growth-promoting rhizobacterium
753 *Paraburkholderia phytofirmans* PsJN. *Appl Environ Microbiol* 2016; 83(1).
754 <https://doi.org/10.1128/AEM.01991-16>
- 755 36. Burton J, Martinez C, Curley R. *Methods of testing and suggested standards for*
756 *legume inoculants and preinoculated seeds*. Milwaukee, Wisconsin, USA, Nitragin
757 Sales Corp, 1972.

- 758 37. Hoagland D, Broyer T. General nature of the process of salt accumulation by roots
759 with description of experimental methods. *Plant Physiol* 1936; 11:471e507.
760 <https://doi.org/10.1104/pp.11.3.471>.
- 761 38. Minamisawa K, Fukai K. Production of indole-3-acetic acid by *Bradyrhizobium*
762 *japonicum*: a correlation with genotype grouping and rhizobitoxine production.
763 *Plant Cell Physiol* 1991; 32(1):1-9.
764 <https://doi.org/10.1093/oxfordjournals.pcp.a078042>
- 765 39. Olesen MR, Jochimsen BU. Identification of enzymes involved in indole-3-acetic
766 acid degradation. *Current Issues in Symbiotic Nitrogen Fixation*. Springer,
767 Dordrecht, 1996, 143-149. https://doi.org/10.1007/978-94-011-5700-1_20
- 768 40. Jarabo-Lorenzo A, Perez-Galdona R, Vega-Hernandez M, Trujillo J, Leon-Barrios
769 M. Indole-3-acetic acid catabolism by bacteria belonging to the *Bradyrhizobium*
770 genus. In *Biological Nitrogen Fixation for the 21st Century, Current Plant Science*
771 *and Biotechnology in Agriculture*, Elmerich C, Kondorosi A, Newton WE (eds),
772 Springer, Dordrecht, 1998, vol. 31, 484-484.
773 https://doi.org/10.1007/978-94-011-5159-7_299
- 774 41. Donati A, Lee H, Leveau J, Chang W. Effects of indole-3-acetic acid on the
775 transcriptional activities and stress tolerance of *Bradyrhizobium japonicum*. *PloS*
776 *one* 2013; 8(10). <https://doi.org/10.1371/journal.pone.0076559>

- 777 42. Scott J, Greenhut I, Leveau J. Functional characterization of the bacterial *iac* genes
778 for degradation of the plant hormone indole-3-acetic acid. *J Chem Ecol* 2013;
779 39(7):942-951. <https://doi.org/10.1007/s10886-013-0324-x>
- 780 43. Shu HY, Lin LC, Lin TK, Chen HP, Yang HH, Peng KC, et al. Transcriptional
781 regulation of the *iac* locus from *Acinetobacter baumannii* by the phytohormone
782 indole-3-acetic acid. *Anton Leeuw Int J G* 2015; 107(5):1237-1247.
783 <https://doi.org/10.1007/s10482-015-0417-3>
- 784 44. Laird T, Leveau J. Finished Genome Sequence of the Indole-3-Acetic
785 Acid-Catabolizing Bacterium *Pseudomonas putida* 1290. *Microbiol. Resour.*
786 *Announc* 2019; 8(28), <https://doi.org/10.1128/MRA.00519-19>.
- 787 45. Sadauskas M, Statkevičiūtė R, Vaitekūnas J, Meškys R. Bioconversion of
788 Biologically Active Indole Derivatives with Indole-3-Acetic Acid-Degrading
789 Enzymes from *Caballeronia glathei* DSM50014. *Biomolecules* 2020; 10(4).
790 <https://doi.org/10.3390/biom10040663>
- 791 46. Collino D, Salvagiotti F, Peticari A, Piccinetti C, Ovando G, Urquiaga S, et al.
792 Biological nitrogen fixation in soybean in Argentina: relationships with crop, soil,
793 and meteorological factors. *Plant Soil* 2015; 392:239–252
794 <https://doi.org/10.1007/s11104-015-2459-8>
- 795 47. Mengucci F, Dardis C, Mongiardini E, Althabegoiti M, Partridge J, Kojima S, et al.
796 Characterization of FliL Proteins in *Bradyrhizobium diazoefficiens*: Lateral FliL

797 Supports Swimming Motility, and Subpolar FliL Modulates the Lateral Flagellar
798 System. J Bacteriol 2020; 202(5):e00708-19. <https://doi.org/10.1128/JB.00708-19>
799 48. Bronstein P, Marrichi M, Cartinhour S, Schneider D, De Lisa M. 2005.
800 Identification of a twin-arginine translocation system in *Pseudomonas syringae* pv.
801 Tomat DC3000 and its contribution to pathogenicity and fitness. J. Bacteriol.
802 187:8450-8461. <https://jb.asm.org/content/187/24/8450>

803

804 **Legends to figures**

805 **Fig. 1.** Evolution of IAA concentration ($\mu\text{g}\cdot\text{ml}^{-1}$) measured along time (h) in (A) YEM
806 (Yeast Extract Mannitol) culture medium, *BjE109*, *BdUSDA110* and *BeSEMIA5019*
807 cultures modified by the exogenous addition of IAA to a final concentration of 40
808 $\mu\text{g}\cdot\text{ml}^{-1}$. (B) Supernatants and heat denatured supernatant of *BjE109* modified by the
809 exogenous addition of IAA to a final concentration of 40 $\mu\text{g}\cdot\text{ml}^{-1}$. Values shown are
810 mean \pm SD (n = 3). Where not shown, the SD was smaller than the symbol.

811

812 **Fig. 2.** IAA concentration ($\mu\text{g}\cdot\text{ml}^{-1}$) measured along time (h) in *BjE109* cultures
813 modified by the exogenous addition of IAA to a final concentration of 0, 20, 40, 80, 120
814 and 160 $\mu\text{g}\cdot\text{ml}^{-1}$ of IAA ($\mu\text{g}\cdot\text{ml}^{-1}$) per tube. Values shown are mean \pm SD (n = 3). Where
815 not shown, the SD was smaller than the symbol.

816

817 **Fig. 3.** IAA concentration ($\mu\text{g}\cdot\text{ml}^{-1}$) measured along time (h) in supernatants of *BjE109*
818 cultures obtained from early exponential (EE) or late exponential (LE) growth phase
819 modified by the addition of an IAA solution to a final concentration of $40 \mu\text{g}\cdot\text{ml}^{-1}$.
820 Values shown are mean \pm SD ($n = 3$). Where not shown, the SD was smaller than the
821 symbol.

822

823 **Fig. 4.** IAA concentration ($\mu\text{g}\cdot\text{ml}^{-1}$) measured along time (h) in *BdUSDA110* wild type,
824 *BdUSDA110 Δ iacA* and *BdUSDA110 Δ iacC* mutant modified by exogenous addition of
825 IAA to a final concentration of $40 \mu\text{g}\cdot\text{ml}^{-1}$. Values shown are mean \pm SD ($n = 3$). Where
826 not shown, the SD was smaller than the symbol.

827

828 **Fig. 5.** IAA concentration ($\mu\text{g}\cdot\text{ml}^{-1}$) measured along time (h) in *BjE109* wild type and
829 *BjE109 Δ iacC* mutant modified by exogenous addition of IAA to a final concentration of
830 $40 \mu\text{g}\cdot\text{ml}^{-1}$. Values shown are mean \pm SD ($n = 3$). Where not shown, the SD was smaller
831 than the symbol.

832

833 **Fig. 6.** Metabolic products identified after heterologous expression of the *iacCD*
834 construct in *C. pinatubonensis* JMP134. The figure represents the putative degradation
835 pathway in *BjE109* in relation of the identified metabolites (blue color) and the ones
836 expected (red color) in our experiments.

1 **Table 1:** Strains, plasmids and primers

Strains, plasmid and primers	Relevant characteristics	Reference or source
Strains		
<i>B. japonicum</i> E109 (<i>Bj</i> E109)	degrade IAA	WDCM31 ^(a)
<i>B. diazoefficiens</i> USDA110 (<i>Bd</i> USDA110)	degrade IAA	[18]
<i>B. japonicum</i> E109 Δ <i>iacC</i> (<i>Bj</i> E109 Δ <i>iacC</i>)	unable to degrade IAA	This study
<i>B. diazoefficiens</i> USDA110 Δ <i>iacC</i> (<i>Bd</i> USDA110 Δ <i>iacC</i>)	unable to degrade IAA	This study
<i>B. diazoefficiens</i> USDA110 <i>spc4</i> (<i>Bd</i> USDA110 Δ <i>iacA</i>)	degrade IAA	[16]
<i>B. elkanii</i> SEMIA 5019 (<i>Be</i> SEMIA5019)	produce IAA, unable to degrade IAA	EMBRAPA -CNPAB
<i>B. japonicum</i> E109 Δ <i>iacC</i> /pJN105 <i>iacC</i>	degrade IAA	This study
<i>Cupriavidus pinatubonensis</i> JMP134	unable to use IAA as a sole carbon and energy source	[35]
Plasmids		
pK18mobSacB	<i>lacZ</i> α Km ^r <i>sacB</i>	[19]
pK18Sac:: <i>iacCBd</i>	<i>lacZ</i> α Km ^r <i>sacB</i> carrying the internal fragment of <i>iacC</i> from <i>Bd</i>	This study
pK18Sac:: Δ <i>iacCBd</i>	<i>lacZ</i> α Km ^r <i>sacB</i> carrying the internal fragment of <i>iacC</i> from <i>Bd</i> deleted in SalI sites	This study
pK18SacB:: <i>iacCBj</i>	<i>lacZ</i> α Km ^r <i>sacB</i> - <i>iacC</i> carrying the internal fragment of <i>iacC</i> from <i>Bj</i>	This study
pK18Sac:: Δ <i>iacCBj</i>	<i>lacZ</i> α Km ^r <i>sacB</i> - <i>iacC</i> carrying the internal fragment of <i>iacC</i> from <i>Bj</i> deleted in SalI sites	This study
pJN105 (pBBR)	Gm ^r	[20]
pBS1	broad host range gateway destination vector, <i>araC</i> -P _{BAD} , Gm ^R	[48]
Primers		
FW <i>iacCE</i> (EcoRI)	AAAAgaattcGCTGGGTCTATGTCGGGC	This study
RV <i>iacCH</i> (Hind III)	AAAaagcttGACCTGCCACTGCATCGT	This study
FWext	TCCTCAGCGACGACGAGA	This study
RVext	TTCAGGAGCAGCAGGTCC	This study

2 ^(a) IMYZA-Instituto de Microbiología y Zoología Agrícola. Castelar. Argentina

Table 2. Effects of inoculation with *BjE109*, *BdUSDA110* and *iacC* mutants on soybean seedlings growth and nodulation. Different letters represent significant differences according to Tukey test $p < 0.05$. Numbers in **bold** represent the difference percentages between mutants and wild type strain.

	MRN	SRN	RN	SDW	RDW
Control	nd	nd	nd	0.21±0.007 ^d	0.048±0.009 ^d
E109	11.68±0.29 ^b	9.14±0.62 ^a	20.83±0.61 ^b	0.33±0.008 ^a	0.073±0.004 ^b
E109 <i>ΔiacC</i>	8.68±0.38 ^c	7.64±0.83 ^{ab}	16.32±0.91 ^c	0.27±0.009 ^b	0.057±0.011 ^c
	-25.6%	-16.4%	-21.6%	-18.05%	-21.9%
USDA110	22.66±0.3 ^a	3.22±0.71 ^b	25.88±0.34 ^a	0.29±0.004 ^b	0.080±0.007 ^a
USDA110 <i>ΔiacC</i>	12.94±0.47 ^b	2.09±0.57 ^b	15.04±0.52 ^c	0.23±0.003 ^c	0.072±0.015 ^b
	-42.8%	-35.0%	-40.4%	-20.6%	-8.75%

References: **MRN**: Main root nodules.plant⁻¹; **SRN**: Secondary root nodules.plant⁻¹; **RN**:

Root nodules.plant⁻¹; **SDW**: Shoot dry weight.plant⁻¹; **RDW**: Root dry weight.plant⁻¹ (36).

nd: not determined.

Figure 1

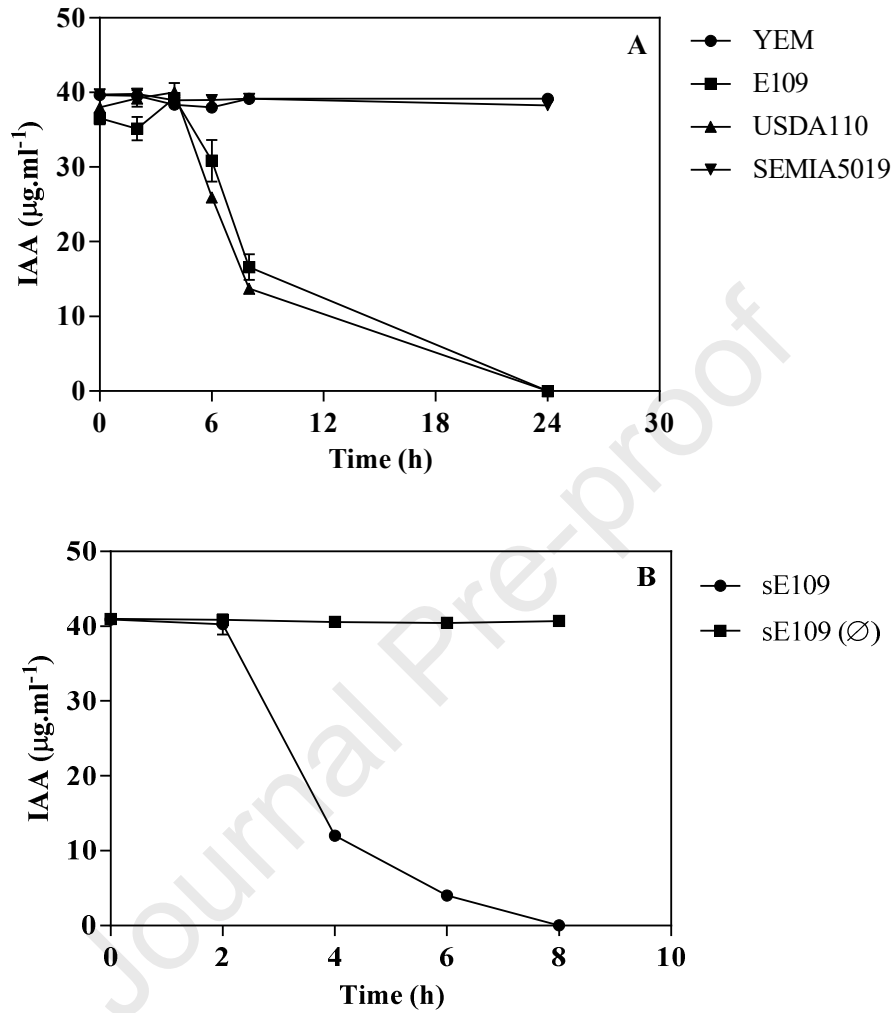


Figure 2

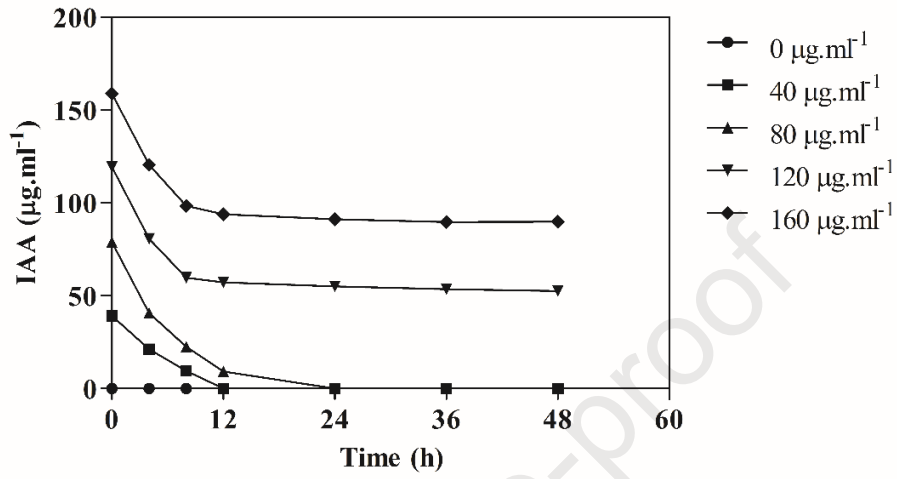


Figure 3

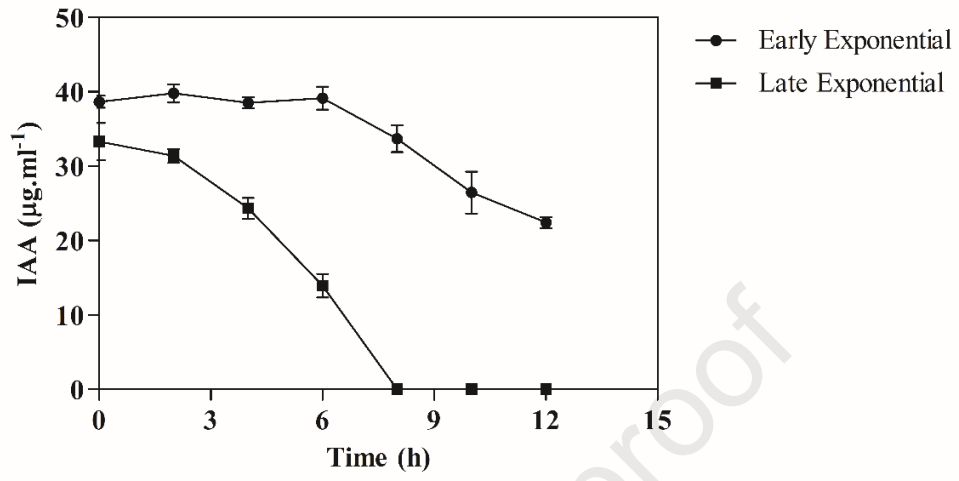


Figure 4

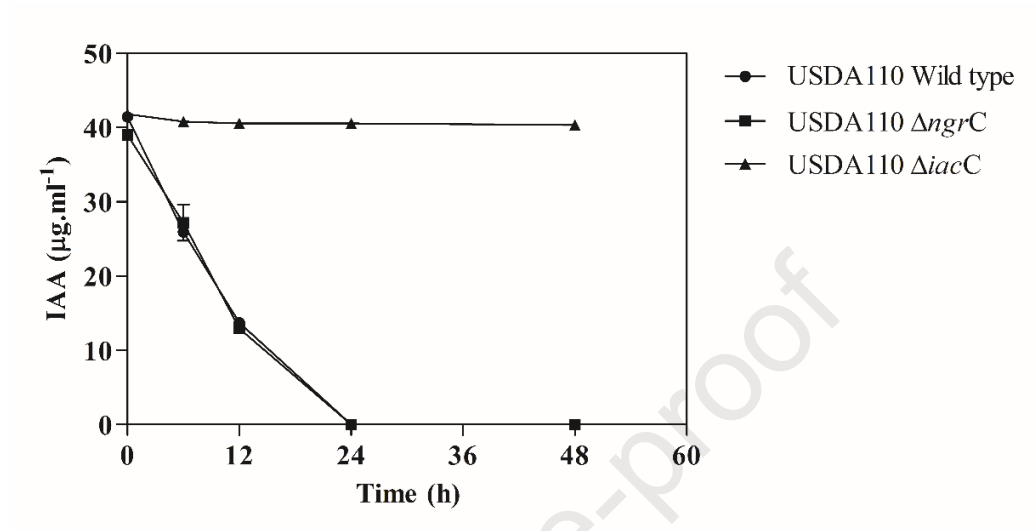


Figure 5

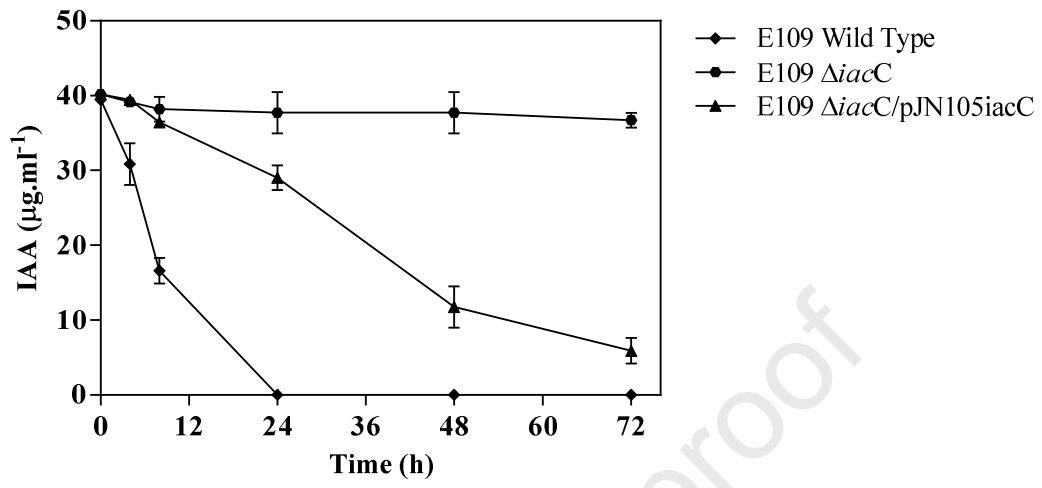


Figure 6

